REPORT DOCUMENTATION PAGE

Form Approved
OMB NO. 0704-0188

1. AGENCY USE ONLY (Leave Blank)	2. REPORT DATE	3. REPORT TYPE AND DATES COVERED
	7th November 2005	Final 1st May 2001 to 31st Jan 2005

4. TITLE AND SUBTITLE	5. FUNDING NUMBERS
Silicon Quantum Information Processing FInal Report	DAAD19-01-1-0552
6. AUTHOR(S) Dr D.J. Paul	
7. PERFORMING ORGANIZATION NAME(S) AND ADDRESS(ES) University of Cambridge, Cavendish Laboratory, Madingley Road, Cambridge, CB3 0HE, U.K.	8. PERFORMING ORGANIZATION REPORT NUMBER Final Report
9. SPONSORING / MONITORING AGENCY NAME(S) AND ADDRESS(ES) U. S. Army Research Office P.O. Box 12211 Research Triangle Park, NC 27709-2211	10. SPONSORING / MONITORING AGENCY REPORT NUMBER 42381.1-PH-QC

11. SUPPLEMENTARY NOTES

The views, opinions and/or findings contained in this report are those of the author(s) and should not be construed as an official Department of the Army position, policy or decision, unless so designated by other documentation.

12 a. DISTRIBUTION / AVAILABILITY STATEMENT	12 b. DISTRIBUTION CODE
Approved for public release; distribution unlimited.	

13. ABSTRACT (Maximum 200 words)

C0Ä?

The following results are presented:

1. Electronic measurements of sodium impurity states
2. T_2 lifetime measurements using EPR

14. SUBJECT TERMS	15. NUMBER OF PAGES
	12
	16. PRICE CODE

17. SECURITY CLASSIFICATION OR REPORT	18. SECURITY CLASSIFICATION ON THIS PAGE	19. SECURITY CLASSIFICATION OF ABSTRACT	20. LIMITATION OF ABSTRACT
UNCLASSIFIED	**UNCLASSIFIED**	**UNCLASSIFIED**	**UL**

NSN 7540-01-280-5500

Standard Form 298 (Rev.2-89)
Prescribed by ANSI Std. 239-18
298-102

Enclosure 1

UNIVERSITY OF CAMBRIDGE

Silicon Quantum Information Processing

Contract: DAAD190110552

Final Report
1st January 2003 to 31st August 2004

Prime contractor: University of Cambridge, U.K. Sub-contractor: Hunter College, CUNY, U.S.A.

1. Scientific Objectives

The initial aim of the programme was to demonstrate three qubits using Na donors in Si MOSFETs by the end of the programme. The initial objectives can be summarised as follows:-

2.1 Fabricate a single electron transistor using AFM lithography on the gate of a MOSFET. This is the detector for the qubits.

2.2 Fabricate a MOSFET with a determined number of Na^+ donors in the oxide.

2.3 Fabricate and detect the positioning of a single Na+ ion in a predetermined position to allow fabrication of qubits.

2.4 Measure the T_2 decoherence time for Na in Si using the temperature dependence of the impurity band and spin dependent scattering.

2.5 Provide a model for the Na donor fabrication.

2. Summary of Important Results

2.1 Electronic Transport

Since the invention of the silicon MOSFET, understanding the influence of impurities, especially sodium contamination, on device performance has been a priority and continues to provide a rich system for investigation by experimental and theoretical physicists alike. The electronic properties of sodium doped MOSFETs were first studied by Fowler and Hartstein [1,2] in the 1970s. They reported a single, broad peak in the subthreshold drain current against gate voltage and attributed it to the formation of an impurity band induced by the presence of sodium ions near the Si-SiO_2 interface. Further studies of narrow channel devices (~100 nm) demonstrated a series of reproducible sharp peaks [3], while later experiments found evidence for resonant tunneling between localised states in the channel. [4,5,6] For sufficiently low impurity concentrations, the overlap between neighbouring localized electron wavefunctions and consequently the hybridisation of their excited states is predicted to be reduced [7], splitting the single impurity band observed at high concentrations into the ground and excited bands as modeled by Ghazali. [8] Increasing the resistivity of the silicon substrate reduces the scattering from acceptors at the Si-SiO_2 interface, allowing the possibility for such a band splitting to be experimentally observed in the transport. In this paper, we will present evidence for the observation of two separate impurity bands with a soft gap, based on analysis of the temperature dependent conductivity below 20 K.

The device we used is a MOSFET fabricated on a (100) oriented p-silicon wafer and was subsequently patterned in the circular Corbino geometry to eliminate Hall voltages and possible leakage paths. The effective gate channel length and interior width were respectively 1 μm and 346 μm. A high resistivity wafer (10^4 Ω.cm) provided a background concentration of less than 10^{12} cm^{-3} of boron corre-

sponding to a mean distance between impurities of 1 μm. A 35 nm gate oxide was grown at 950°C in a dry, chlorine-free oxygen atmosphere. The phosphorous implanted and aluminium sputtered contacts were highly metallic and Ohmic at all temperatures investigated. Sodium ions were introduced onto the oxide surface by immersing the device in a 10^{-7} N solution of high purity sodium chloride (99.999%) in de-ionised water.

The surface of the chip was dried with nitrogen gas and an aluminium gate subsequently evaporated. To observe or remove the low temperature conductivity structures, the mobile ions are drifted through the oxide to the Si/SiO_2 interface, or returned to the $Al\text{-}SiO_2$ interface by applying either a +4 V or a -4 V DC gate-substrate bias for 10 min at 65°C before the device is cooled down to helium temperature at which sodium looses its diffusivity in the oxide. All measurements were performed using standard low-noise lockin techniques with an amplifier of 10^8 V / A. The AC excitation was maintained at 15 μV with a frequency of 11 Hz. Suitable RC filters were employed to eliminate any DC offset from the amplifier. The gate voltage was controlled by a high resolution digital to analog converter. All experiments were performed in a 3He cryostat and the temperature was measured by a calibrated germanium thermometer.

Fig. 1 shows the conductivity σ of our device at 300 mK versus gate voltage V_g for the case where the sodium ions had been drifted to the $Si\text{-}Si0_2$ interface. Two groups of peaks appear clustered around V_g = -2V and -0.5 V and separated by a region of low conductivity and limited by noise. The origin of the peaks themselves will be discussed later. Following a -4 V drift, no structure was detectable over the full range of gate voltages investigated but a difference in threshold voltage of 0.2 V was found at 77 K between the characteristics of the device following + 4 V and -4 V drifts. This was attributed to the presence of mobile charges close to the $Si\text{-}Si0_2$ interface at a concentration of 3.7×10^{11} cm^{-2} corresponding to a mean impurity separation of 16 ± 1 nm. In a reference device where no sodium was introduced, no sub-threshold conductivity peaks and no shift of the threshold voltage appeared for any drift conditions investigated. Tunneling through the

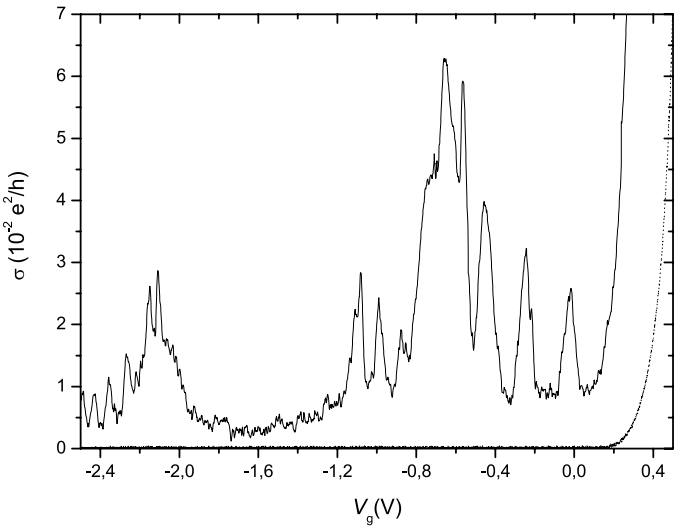

Fig. 1: The source-drain conductivity versus gate voltage at 300 mK following a +4 V drift and a –4 V drift (dotted line).

oxide and other leakage currents were discounted as the gate leakage current was below 50 fA at 4.2 K and was approximately constant over the range of gate voltages used. We remark also that no hysteresis and thus no charging effects that have been reported in similar devices [9] were observed here.

The presence of two distinct ranges of V_g where peaks appear suggests the possibility of a split impurity band (Fig. 1). Such a splitting into a ground and an excited state is expected to happen for low-doping concentration [8,10] if one takes into account the overlaps between impurity wavefunctions and uses a multi-band formalism [l1]. The conductivity of a Si-MOSFET is not directly related to the density of states and the fact that we see two regions of high conductivity separated by a region of low conductivity is only an indirect indication that the device density of states consists of two bands sep¬arated by a gap. In fact, through the Kubo formalism, conductivity tends to be related to local paths through a disordered device but density of states is a global property. In order to show that the density of states splits into two bands, we have looked at the temperature dependence of the conductivity at a series of different gate voltages. For all gate voltages studied, the conductivity decreases non-monotonically as temperature is lowered (Fig. 2). In the range 1 K to 20 K, we observe the characteristics of hopping conduction so that the conductivity $\sigma(T)$ is fitted to

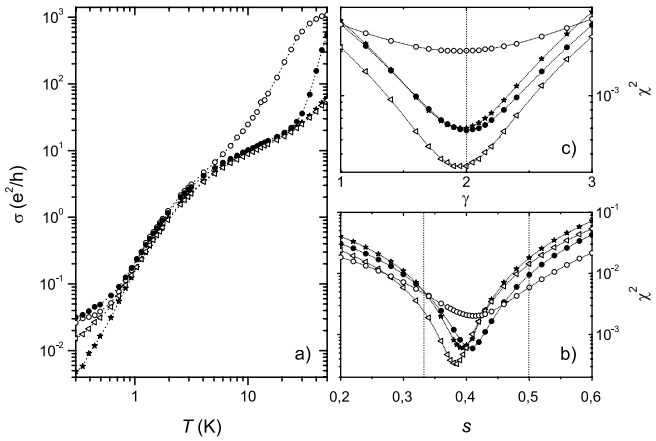

Fig. 2: Temperature dependence of the conductivity for V_g = 0.1 (o), –0.24 (•), –1.48 (*) and –2.26 (◁), b) variation of the reduced χ^2 with s = 0.412, 0.406, 0.394 and 0.385 respectively and c) variation of the reduced χ^2 with γ for s equal to the optimum value found in 2(b), for the appropriate gate voltages, displaying consistency with a minimum at γ = 2 (dotted line). Lines in b) represent the exponent for the Mott hopping regime (left) and Efros Schlovskii regime (right).

the generalised equation:

$$\sigma = \sigma_0 T^{-\gamma s} e^{-\left(\frac{T_0}{T}\right)^s} \qquad (1)$$

where T_0 and σ_0 depend on gate voltage.

The best values for γ and s are found by minimizing the value of the reduced chi-square deviation χ^2 with standard procedures. Figs 2(a)- (b) show the optimum values determined for four gate voltages, one point in the threshold region (V_g = 0.1 V), the upper band (V_g = -0.24 V), the gap (V_g = -1.48 V) and the lower band (V_g = -2.26 V). The resulting fits for σ(T) are valid over three orders of magnitude in σ (Fig. 3). Studies in gate voltage show that γ = 1.98 ± 0.04 and s = 0.39 ± 0.02 for V_g below 0.25 V. Above this point, the value of s decreases rapidly towards s = 1/3 for T ≥ 4K and the range is better described by Mott hopping conduction [12]. It is worth noticing that the smallest values of s are obtained for band centre regions -0.8 V < V_g < -0.5 V and -2.2 V < V_g < -2.1 V for which the hopping lengths are relatively smaller and the Coulomb interactions weaker.

We emphasise that the use of temperature dependent exponential prefactors allows the fine distinction between Mott (s = 1/3), Efros-Schklovskii (s = 1/2) [13] and the regime under study

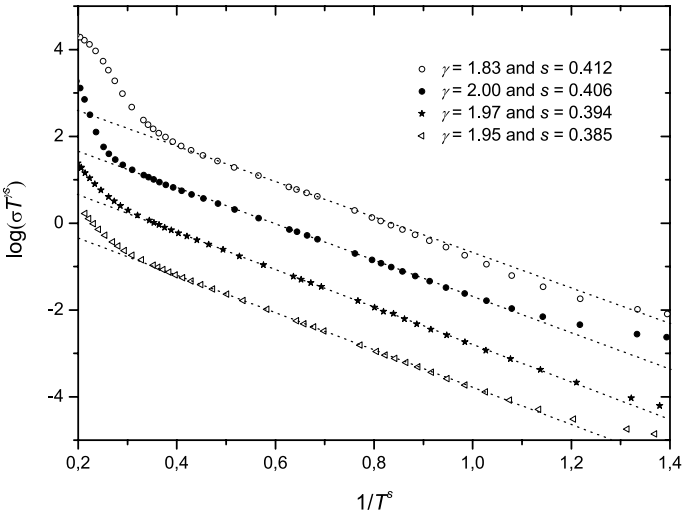

Fig. 3: Temperature dependence of the conductivity for V_g = 0.1 (o), –0.24 (•), –1.48 (*) and –2.26 (◁) for the optimum values of g and s defined in Eq. 1. For clarity, curves are shifted downwards respectively by 0, 1, 2 and 3 from their original values.

(s ~ 0.39). The finding that γ ~ 2 is consistent with the formulation for σ(T) given by Allen and Adkins [14,15] if it is rederived for the 2D case. This gives the conductivity in terms of both the localization length ξ and the density of states at the Fermi level $n(E_F)$. Accounting for the fact that Coulomb interactions between electrons in different localized states modifies the density of states close to the Fermi level so that $n(E) = N_0 | E - E_F |^p$, we obtain:

$$\sigma = \sigma_0 T^{-\gamma\left(\frac{p+1}{p+3}\right)} e^{-\left(\frac{T_0}{T}\right)^{\frac{p+1}{p+3}}} \text{ with } \gamma = 2 \qquad (2)$$

$$\sigma_0 = A_0 \left[\pi^2 N_0^2 \xi^{3p+13} (p+1)^{p-3}\right]^{frac-1p-} \qquad (3)$$

$$k_B T_0 = \frac{p+3}{p+1}^{\frac{p+3}{p+1}} \left[\frac{(p+1)^3}{\pi N_0 \xi^2}\right]^{\frac{1}{p+1}} \qquad (4)$$

where A_0 is a constant depending on the electronic properties of bulk silicon and k_B the Boltzmann constant.

The conditions given by Allen [14] for the use of the equations Eqs. 2-4 are satisfied in our device. Recent calculations showed that sodium ions in the oxide may trap either one or two valence electrons against the Si/SiO_2 interface and that the wavefunctions of the localized states remain hydrogen-like.

[16] Also, hopping conduction is present in our device so that the only mobile electrons are found in an energy band corresponding to a hopping energy around the Fermi level. The resulting Coulomb gap for s = 0.39 (i.e. $n(E) \sim | E - E_F |^{0.30}$) is much sharper than for the Efros regime where $n(E) \sim | E - E_F |$. This behaviour has been predicted by Blanter and Raikh [17] while studying 2D systems localized by disorder. They have shown that a metallic gate close to the interface provides image potentials that modify the densityofstates to the form $n(E) = n(E_F)+N_0 |E-E_F|^{1/3}$ at T = 0 K and thus gives an exponential dependence of $T^{-0.4}$ for the conductivity. This behaviour is explained by the fact that the oxide thickness plays the role of the screening length and that initial and final states become electrostatically independent at low temperature when the hopping length R becomes greater than twice the oxide thickness d. This then produces a crossover from the Efros to the Mott regime. The localization length in our device was approximately estimated by fitting the conductivity with p = 0, using the Mott formula for $k_B T_0$ and taking the 2D value for the density of states. For V_g = -0.4 V, this gives $\xi \sim 20$ nm and a hopping length $R \sim 63$ nm at 1 K. Our device has a gate oxide of d = 35 nm and the Coulomb interactions may be screened by the electrostatic gate as $R \sim 2d$. This demonstrates the device may well be in the regime described by Blanter and Raikh. Fits of the conductivity using $\gamma = 2$ and s = 0.4 are still valid for V_g smaller than 0.25 V and from 1 K to 18 K typically, so we will proceed with these values. In this regime, the density of states at E_F is given by :

$$n(E_F) = n_0(E_F) - \frac{2\pi n_0(E_F)^2 de^2}{4\pi\epsilon_0\epsilon_r}\nu \qquad (5)$$

$$n_0(E_F) = \left(\frac{N_0}{2\pi}\right)\left(\frac{4\pi\epsilon_0\epsilon_r}{2d^2d^2}\right)^{\frac{1}{3}} \qquad (6)$$

where ε_r is the permittivity of silicon.

These equations have been derived at T = 0 under the condition that $n(E_F)d^2V(d)$ (< 0.095 in our device) is small where V is the impurity Coulomb potential. At higher temperature but for T « V(d), the gap is partly filled. The Coulomb interactions then become negligible for energies below V(2d) and the density of states saturates such as $n_0(E_F) = n_0(E_F + V(2d))$.[18] This condition decreases the value of ν from 1 down to 0.11. Combining (3) and (4), the parameters N_0 and ξ were expressed in terms of T_0 and σ_0, values easily accessed experimentally. The density of states was extracted using equation (5) and (6). Several values of Ξ are found in the literature [19] but the most recent value was found by Martin [20] who gives Ξ = 16.14eV implying $A_0 = 1.10 \times 10^{-3}\ e^2.h^{-1}.K^{-0.8}$.

The density of states is shown in Fig. 4. The value we find is two orders of magnitude lower than the pure 2D case (‘” $1.6 \times 10^{14}\ eV^{-1}.cm^{-2}$ with valley degeneracies). The large background is predominantly due to the conduction band tail which spreads over the full range of V_g studied. The upper band also has a significant tail. The presence of density of states tails is a common occurance in disordered systems with low impurity concentration and localized wavefunctions [21,22,23] but its linear shape for $V_g < 0$ V is unusual. It has been attributed to the formation of regions of constant local potential energy at the Si-SiO_2 interface and containing a random number of charges. [24] Two regions of higher density are superimposed on the background density and correspond to the upper and lower groups of peaks. This confirms that the structure observed in the conductivity is due to the pres¬ence of two separate bands. By numerically

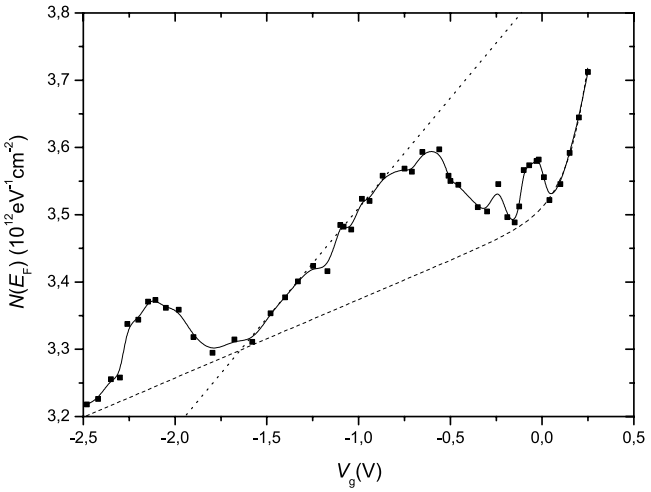

Fig. 4: Variation of the density of states at E_F with gate voltage. The dashed and dotted lines represent respectively the background density due to the conduction band tail and the upper band tail.

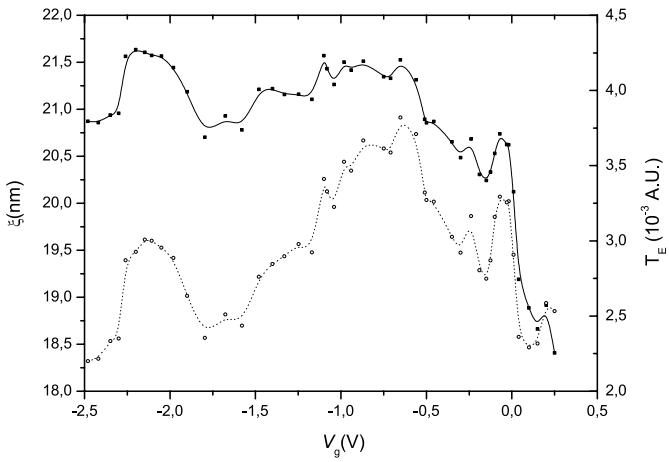

Fig. 5: Variation of the localisation length (•) and the trnasmission coefficient at 1 K (o) with gate voltage.

subtracting the background density and integrating over the appropriate gate voltage and by supposing a linear relation between the gate voltage and the surface potential energy, we estimate the upper band contains approximately 3 times the number of states as the lower band. This value is an upper bound as energetically deeper states could not be accessed experimentally.

The variation of the localization length ξ (Fig. 5) follows that of the density of states, showing the two bands do correspond to the more conductive regions. The value of ξ decreases rapidly when approaching the threshold voltage. This is expected as the region between $V_g = 0$ V and $V_g = 0.4$ V is both in the band tails of the conduction band and the upper band, the conduction band edge being well above 0.4 V. Thus, this region is still a region of strong localization. Nevertheless, the value of ξ is expected to rise once the Fermi energy crosses the conduction band edge. Finally, taking into account fitting errors as well as the discrepancy in the value of the deformation potential, we estimate the localization length within 5 % and the density of states within 6 %. From the same derivation which gave (1), (2) and (3), the transmission coefficient is obtained:

$$\ln\left(T_E\right) = -\frac{2}{p+3}\left(\frac{T_0}{T}\right)^{\frac{p+1}{p+3}} \qquad (7)$$

The experimental variation of the transmission coefficient in gate voltage (Fig. 5) shows that the conductivity of the two bands mostly comes from the higher mobility of the states of energies within the upper and lower bands and less from the increase in the density of states.

In conclusion, we have observed in electrical transport measurements, an unusual hopping regime with an exponent 0.4 which results from the screening of the Coulomb interactions by the metal gate. We have shown that, consequently, both the localization length and the density of states can be extracted from the temperature dependence of the conductivity. This analysis has given strong evidence for the existence of two separate bands and a soft gap at low temperature. This may result from the splitting of the impurity band into a lower and an upper band in presence of Coulomb interactions. The formation of the two bands results itself from the presence of a low concentration of sodium impurities close to the Si-SiO_2 interface. The conditions for the observation of such a formation may be the creation of deep but well separated impurity potentials at the interface, resulting in electron localization. Finally, the electron screening may be sufficiently weak and the disorder not too strong to allow a Mott-Hubbard transition to take place. The two bands could then possibly be Hubbard bands.

2.2 Electron Paramagnetic Resonance

A commercial Brüker EMX spectrometer was used for the measurements. To increase sensitivity, a modulated field ΔB_{mod} is applied at frequency ω_{mod} in addition to the dc microwave power. The Brüker was used with a modulated frequency of 100 kHz and the modulation amplitude was set to be sufficiently small to prevent additional broadening. The lineshape is assumed to relax between successive passes of the microwave resonance condition. In the case of homogeneous broadening, the linewidth arises solely due to T_1 and T_2 relaxation processes at the EPR centres. A continuous flow cryostat allows the sample inside the microwave cavity to be cooled down to about 10 K while radiation of frequency 9.2 GHz is applied and measured with a HP53151A frequency counter.

A batch of MOSFETs with 210 nm gate oxides was prepared and dipped in 10^{-5} M NaCl solution

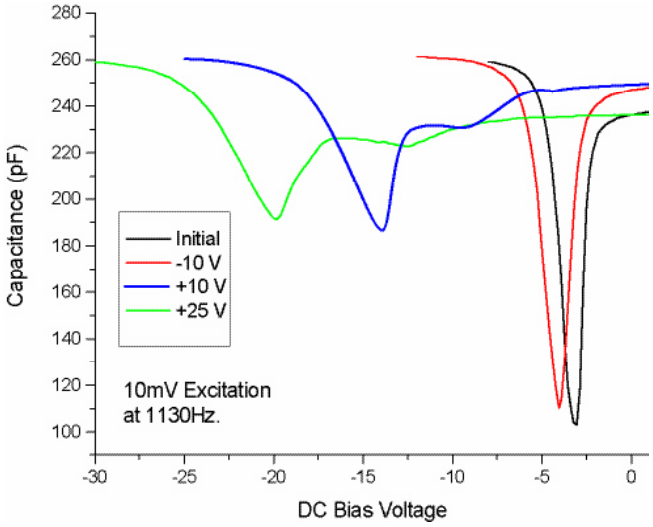

Fig. 6: A MOSFET capacitor dipped in 10^{-5} M solution of NaCl. A –12.9 V threshold shift is observed with +10 V corresponding to a $1.32x10^{12}$ cm^{-2} sodium density.

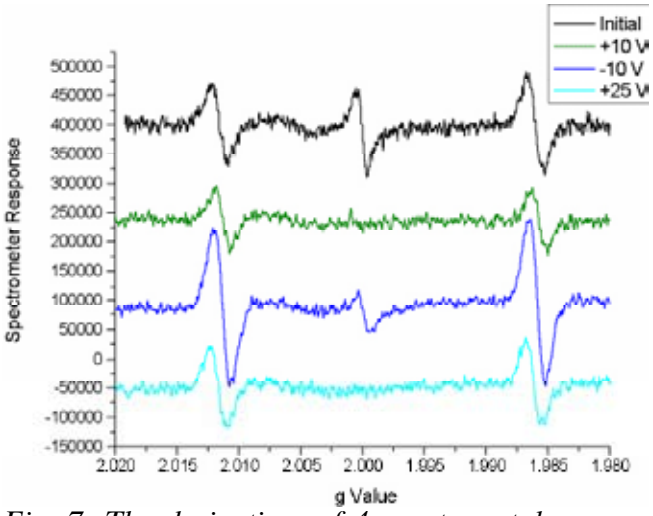

Fig. 7: The derivatives of 4 spectrum taken on a single sample for the last run at 10 K (off set vertically for clarity). The two peaks symmetrical around g=1.9992 are from P impurities. The central peak is close to the free electron value of g=1.99869.

($1.32x10^{12}$ cm^{-2} Na from CV of Fig. 6). The derivative of some of the spectra are shown in Fig. 7 about 6 days after the Na was put into the oxide. The intial spectrum shows two phosphorus peaks symmetrical around g=1.9992 and split by 41.94 Gauss due to the hyperfine interaction with the ^{31}P nucleus [25]. This must be phosphorus in the substrate at ~10^{13} cm^{-3} concentrations even though the substrates are p-type to $5x10^{14}$ cm^{-3}. Around g~2 there is a peak close to the electron g-value. After applying + 10 V the peak disappears and then reappears after –10 V bias. A further positive bias results in the peak disappearing.

Again this peak may be due to electrons from the sodium impurity band but also it may be due to defects at the Si/SiO_2 interface. Fig. 8 demonstrates the diffusion of Na in the gate oxide of a MOSFET after the 6 days from fabrication. If a diffusion constant of 2×10^{-16} cm^2/s is used then a significant amount of Na can diffuse to the oxide interface. While data exists in the literature, there is a large spread in the diffusivities with data ranging from 2.8×10^{-15} m^2/s to 10^{-19} m^2/s. Clearly there is sodium at the Si/SiO_2 interface after 6 days if the higher diffusivity is used and therefore it is possible that the initial measurement in Fig. 7 could be from a sodium impurity band. The +10 V would take the MOSFET into strong inversion with a carrier density of 2.6 x 10^{12} cm^{-2} which is over twice the Na impurity density measured by CV. While EPR resonances from inversion layers have been observed, they are typically a sharp downward peak in the derivative with two smaller satellite peaks [25]. These inver-

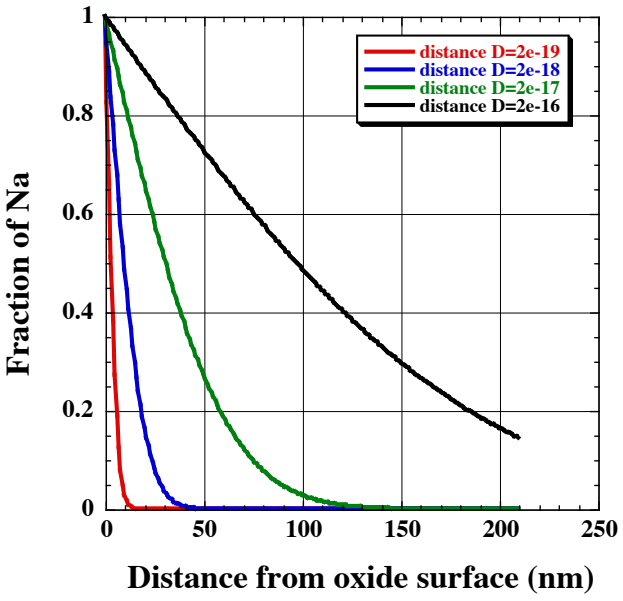

Fig. 8: The concentration of Na in the gate oxide of the MOSFET as a function of distance from the Aluminium gate for 4 diffusivities. Even at the Si/SiO_2 interface which is 210 nm below the surface, a finite amount of sodium has diffused after 6 days.

sion layer peaks are clearly not observed at +10 V, 0 V or –10 V. The threshold voltage for this device is –10.4 V. Therefore measuring at –10 V would have the Fermi energy just above the sodium impurity band but without any significant formation of a high density inversion layer.

The calculated wavefunction has a p-like orbital and therefore there can be no hyperfine interaction with the nuclear spin of the I=+3/2 sodium nucleus. If a hyperfine interaction was present, four resonances would be observed. As the hyperfine interaction is the limiting factor for T_2 in phosphorus doped Si, this may be beneficial for the present sodium system. This also means that no hyperfine splitting of the any peak from electrons in the sodium impurity band should be expected from interactions with the I=+3/2 nuclear spin of ^{23}Na which is the most abundant isotope of sodium.

It is also possible that the resonance in Fig. 7 is due to defects at the Si/SiO_2 interface [26-28]. The main interface defect peak is due to the p_{b0} which has a g-value of 2.006 for the [100] orientation of the present sample. Fig. 9 shows the integrated lines from Fig. 7 and the p_{b0} peak can be observed at 2.006. The g-values for this graph have been calibrated to the correct positions using the two phosphorus peaks which are symmetrical around g=1.9992 ± 0.0494. The p_{b0} peak is therefore the broad resonance around 2.006 and a sharp resonance remains at 1.998 with a T_2^* of 142 ns. The only other known defect state is the E' centre [29] which is centred at g=2.0011. This peak has been shown to saturate at μW powers and the present measurements demonstrate the peak at mW powers where the defect should not be observed. In addition extreme measures such as high temperature anneals in O_2 or γ radiation had to be used to form such defects. All this evidence strongly suggests that the sharp peak around 1.998 is due to electron spins from the sodium impurity band. The only other posibility is that an unknown Si/SiO_2 impurity state due to charge in the oxide might create some line at this particular value. No such states have been observed before and if such a state was created it would probably be the result of the sodium in the oxide.

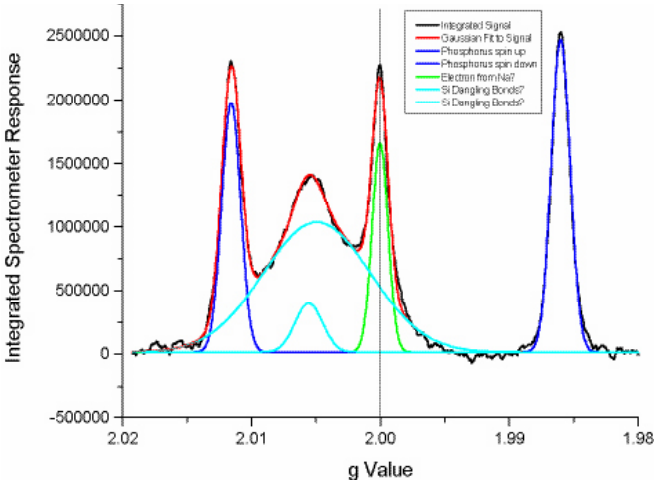

Fig. 9: The integrated lines from Fig. 12 with a number of curves fitted to the data.

Fig. 10 shows the Vogt function fitted to the potential sodium impurity band peak at g=1.998. From the width of this fit, the inverse gives the lower bound for the T_2 lifetime [25] to be 0.5 μs (see Fig. 11 for a description of T_2 and T_2^*). Recently new pulsed EPR measurements of phosphorous doped silicon have appeared in the literature []. Using isotopically purified silicon with a phosphorus concentration of 10^{15} cm^{-3} a T_2 lifetime of 14 ms has been measured at 7 K. One potential issue is that the present technique being employed cannot detect T_2 lifetimes longer than 100 μs. Therefore if T_2 for electrons in the sodium impurity band is as long as most of the other shallow donors in silicon, the present technique cannot measure it unless T_2

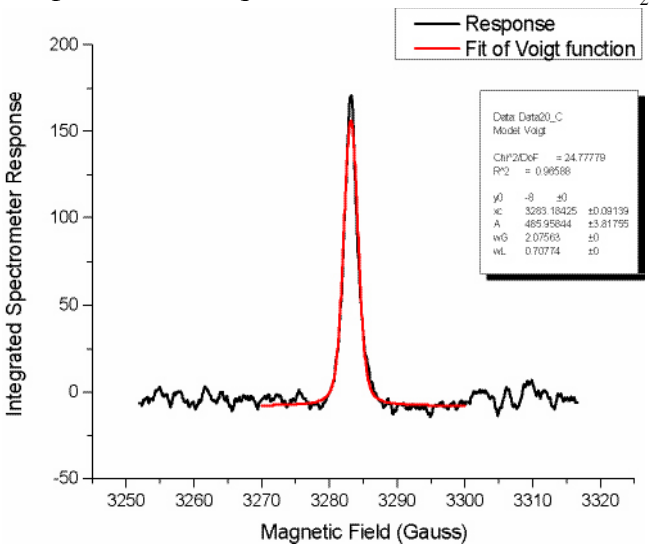

Fig. 10: The Voigt function fitted to the potential sodium impurity band peak at g=1.998 to obtain T_2. The extracted T_2 from this is > 0.5 µs for electrons 5.2 nm apart.

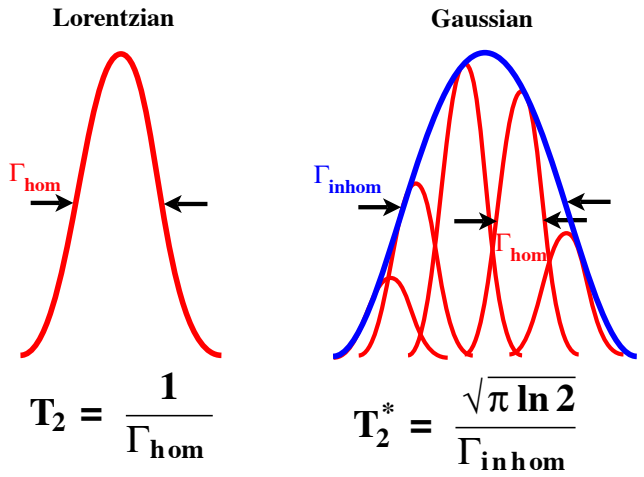

Fig. 11: The difference between homogenously and inhomogenously broadened EPR peaks and the extraction of the appropriate lifetime.

is reduced by moving to higher temperatures. High temperature measurements were also taken for the last set of samples. the phosphorus peaks were observed up to high temperatures but no other peaks became observable at higher temperatures around g=1.99869.

In summary, in two sets of measurements we have achieved a signal which is close to the expected resonance at g=1.99869 and obtained a lower bound for the T_2 lifetime from these resonances of 0.5 μs for a sodium density of 1.32 x 10^{12} cm^{-2}. The state is not hyperfinely split as expected from a p-orbital wavefunction and does not correspond to any of the known interface defect resonances. The spacing of electrons for the lowest density we have managed to measure is only 5.2 nm which is still close to the Bohr radius and hence exchange interactions between the electrons will still be quite strong and therefore reduce the T_2 lifetime. For qubits, this electron spacing will be significantly larger and the exchange interaction should be much smaller. Also it is the Orbach process which typically limits the T_2 lifetime in semiconductors and this has a T^7 temperature dependence [30]. Therefore operating a quantum computer below 1 K should allow significantly higher T_2 lifetimes to be achieved than the 0.5 μs measured in the present results.

6. Publications

(a) Papers published in peer reviewed journals

T. Ferrus, R. George, C.H.W. Barnes, N. Lumpkin, D.J. Paul and M. Pepper, "*Evidence for mulitple impurity bands in sodium-doped silicon MOSFETs*" Submitted to Physical Review B - published on cond-mat/0510145.

(b) Papers published in non-peer reviewed journals or in conference proceedings

None

(c) Papers presented at meetings, but not published in conference proceedings

C.H.W. Barnes, "Quantum computing using electrons trapped in semiconductors". Queen Mary College, London (2002)

C.H.W. Barnes, Quantum computing using electrons trapped in semiconductors. Hewlett Packard Laboratories, Bristol (2002)

C.H.W. Barnes, Quantum Computation Using Sodium atoms Trapped at an Si/SiO2 Interface. 2nd International Workshop on Solid-State Implementations for Quantum Computing IBM Watson Research Center, Yorktown Heights, NY. April (2002)

C.H.W. Barnes, Solid State Quantum Computation. JAPAN-UK 10 +10 MEETING "Semiconductor Physics and Devices" Department of Physics, University of Durham, UK 2-4 August (2002)

D.J. Paul, "Silicon quantum information processing" Quantum Information Processing Workshop, Trinity College Dublin, Ireland, September (2002)

C.H.W. Barnes, Solid State Quantum Computation. Quantum Information Group,Department of

Applied Mathematics and Theoretical Physics, Cambridge 29th October (2002).

C.H.W. Barnes, Static and Dynamic quantum processors Imperial College, London (2003)

C.H.W. Barnes, Solid-State static and dynamic quantum processors University of Leeds (2003)

C.H.W. Barnes, The future of quantum computation THINQC ARDA Harpers Ferry June (2003)

D.J. Paul, "Quantum computing with MOSFETs" University of Cambridge Industrial Open Day, May (2004)

C.H.W. Barnes, Implementing a controllable many-particle system, Quantum Condensates Cambridge July (2005)

(d) Manuscripts submitted, but not published

None

(e) Technical reports submitted to ARO

Quarterly Status Reports 1 to 10
Interim Reports 2001, 2002, 2003, 2004
Final Report

7. Scientific Personnel

Prof. Michael Pepper
Dr Douglas J. Paul
Dr Crispin H.W. Barnes
Dr Thierry Ferrus
Dr Nancy Lumpkin
Dr Alex Moroz
Dr Rutzani Nemutudi
Mr Stephen Binning
Mr Richard George - writing PhD
Mr Timur Zainiev - PhD "Quantum Mechanics and the Greedy Algorithm" Nov 2004
Mr Jon Griffiths - writing PhD

8. Report of Inventions

None

9. Bibliography

[1] F. F. Fang, A. B. Fowler, Phys. Rev. 169, 619 (1967)
[2] A. Hartstein, A. B. Fowler, Phys. Rev. Lett. 34, 1435 (1975)
[3] A. B. Fowler, A. Hartstein and R. A. Webb, Phys. Rev. Lett. 48, 196 (1982)
[4] A. B. Fowler, G. L. Timp, J. J. Wainer and R. A. Webb, Phys. Rev. Lett. 57, 138 (1986)
[5] T. E. Kopley, P. L. McEuen and R. G. Wheeler, Phys. Rev. Lett. 61, 1654 (1988)
[6] D. Popovic, A. B. Fowler and S. Washburn, Phys. Rev. Lett. 67, 2870 (1989)
[7] C. Erginsoy, Phys. Rev. 80, 1104 (1950)
[8] A. Ghazali, A. Gold and J. Serre, Phys. Rev. B 39, 3400
(1989)
[9] V. Ioannou-sougleridis, A. G. Nassiopoulou and A. Travlos,
Nanotechnology, 14, 11174 (2003)
[10] J. Serre and A. Ghazali and A. Gold, Phys. Rev. B 39,
8499 (1989)
[11] J. R. Klauder, Ann. Phys. (N.Y.) 14, 43 (1961)
[12] N. H. Mott, J. Non-Cryst. Solids 1, 1 (1969)
[13] A. L. Efros and B. I. Schklovskii, J. Phys. C 8, L49 (1975)
[14] F. R. Allen and C. J. Adkins, Phil. Mag. 26, 1027 (1972)
[15] R. Mansfield, S. Abboudy and P. Fozooni, Phil. Mag. B
57, 6, 777 (1988)
[16] C. H. W. Barnes and A.V. Moroz, to be published
[17] Y. M. Blanter and M. E. Raikh, Phys. Rev. B 63, 075304
(2001)
[18] I. L. Aleiner and B. I. Shklovskii , Phys. Rev. B 49,13721(1994)
[19] L. J. Sham, Poco Phys. Soc. 81, 934 (1963)
[20] C. Goo Van de Walle and R. M. Martin, Phys.

Rev. B 34, 5621 (1986)
[21] B. I. Halperin and M. Lax, Phys. Rev. 148, 722 (1966)
[22] J. Zittartz and J. S. Langer, Phys. Rev. 148, 741 (1966)
[23] E. O. Kane, Phys. Rev. 131, 79 (1963)
[24] E. Arnold, Appl. Phys. Lett., 25, 705 (1974)
[25] R.S. Alger "*Electron paramagnetic resonance: Techniques and applications*" Interscience Publishers (1968).
[26] J.L. Cantin and H.J. von Bardeleben, J. Non-Crystalline Solids **303**, 175 (2002).
[27] A. Stesmans and V.V. Afanas'ev, J. Appl. Phys. **83**, 2449 (1998).
[28] J.L. Cantin et al., Phys. Rev. B **52**, R11599 (1995).
[29] H. Nishikawa et al., J. Appl. Phys. **65**, 4672 (1989).
[30] A.M. Tyryshkin et al., cond-mat/0303006 and Phys. Rev. B **68**, 193207 (2003).